

1 **Plastid phylogenomics clarifies broad-level relationships in**  
2 ***Bulbophyllum* (Orchidaceae) and provides insights into range evolution**  
3 **of Australasian section *Adelopetalum***

4 **Lalita Simpson<sup>1,2\*</sup>, Mark A. Clements<sup>3</sup>, Harvey K. Orel<sup>4,5</sup>, Darren M. Crayn<sup>1</sup>, Katharina**  
5 **Nargar<sup>1,5</sup>**

6 <sup>1</sup> Australian Tropical Herbarium, James Cook University, Cairns, QLD 4870, Australia

7 <sup>2</sup> College of Science and Engineering, James Cook University, Cairns, QLD 4870, Australia

8 <sup>3</sup> Centre for Australian National Biodiversity Research (joint venture between Parks Australia and  
9 CSIRO, Canberra, ACT 2601, Australia

10 <sup>4</sup> School of BioSciences, The University of Melbourne, Parkville, Victoria 3052, Australia

11 <sup>5</sup> National Research Collections Australia, Commonwealth Industrial and Scientific Research  
12 Organisation (CSIRO), Canberra, ACT 2601, Australia

13 **\* Correspondence:**

14 Lalita Simpson

15 [lalita.simpson1@jcu.edu.au](mailto:lalita.simpson1@jcu.edu.au)

16 **Keywords: Phylogenomics, High-throughput sequencing, Orchidaceae, Divergence time**  
17 **estimation, Ancestral area reconstruction, Australasia, *Bulbophyllum*, *Bulbophyllinae*.**

18

19 **Abstract**

20 The hyper diverse orchid genus *Bulbophyllum* is the second largest genus of flowering plants and  
21 exhibits a pantropical distribution with a center of diversity in tropical Asia. The only *Bulbophyllum*  
22 section with a center of diversity in Australasia is sect. *Adelopetalum*. However, phylogenetic  
23 placement, interspecific relationships, and spatio-temporal evolution of the section have remained  
24 largely unclear. To infer broad-level relationships within *Bulbophyllum* and interspecific  
25 relationships within sect. *Adelopetalum*, a genome skimming dataset was generated for 89 samples,  
26 yielding 70 plastid coding regions and the nuclear ribosomal DNA cistron. For 18 additional samples,  
27 Sanger data from two plastid loci (*matK*, *ycf1*) and nuclear ITS were added using a supermatrix  
28 approach. The study provided new insights into broad-level relationships in *Bulbophyllum*, including  
29 phylogenetic evidence for the non-monophyly of sections *Beccariana*, *Brachyantha*, *Brachypus*,  
30 *Cirrhopetaloides*, *Cirrhopetalum*, *Desmosanthes*, *Minutissima*, *Oxysepala*, *Polymeres* and  
31 *Sestochilos*. Section *Adelopetalum* and sect. *Minutissima* s.s. formed a highly supported clade that  
32 was resolved in sister group position to the remainder of the genus. Divergence time estimations  
33 based on a relaxed molecular clock model placed the origin of *Bulbophyllum* in the early Oligocene  
34 (ca. 33.2 Ma) and of sect. *Adelopetalum* in the late Oligocene (ca. 23.6 Ma). Ancestral range  
35 estimations based on a BAYAREALIKE model identified the Australian continent as ancestral area  
36 of sect. *Adelopetalum*. The section underwent crown diversification during the mid-Miocene to the  
37 late Pleistocene, predominantly in continental Australia. At least two independent long-distance  
38 dispersal events were inferred eastwards from the Australian continent to New Zealand, and New  
39 Caledonia from the early Pliocene onwards, likely mediated by the predominantly westerly winds of

40 the southern hemisphere. Retraction and fragmentation of eastern Australian rainforests from the  
41 early Miocene onwards are discussed as likely drivers of lineage divergence within sect.  
42 *Adelopetalum*, facilitating allopatric speciation.

## 43 1 Introduction

44 The hyper diverse orchid genus *Bulbophyllum* Thouars (Epidendroideae) is the second largest genus  
45 of flowering plants with more than 2,100 species and exhibits exceptional morphological and  
46 ecological diversity (Frodin, 2004; Pridgeon et al., 2014, WCSP 2022). Species of this predominantly  
47 epiphytic genus occur in a wide range of tropical and subtropical habitats, from montane rainforests  
48 to dry deciduous forests, savannah woodlands, and rocky fields with shrubby vegetation (Pridgeon et  
49 al., 2014). *Bulbophyllum* is distributed pantropically, occupying all botanical continents defined by  
50 Brummit (2001) except for Antarctic and Eurasia. The genus is most diverse on the botanical  
51 continent of tropical Asia (1562 species), also occurring on the botanical continents of Africa (305),  
52 temperate Asia (152), Southern America (88), the Pacific (49), Australasia (Australia and New  
53 Zealand; 35), and Northern America (7) (WCSP, 2022). Centres of diversity are found in tropical  
54 Asia in the floristic regions of Malesia (667) and Papuasia (656) and in the Afrotropics in the western  
55 Indian Ocean region, on the islands of Madagascar, and the Mascarenes (218) (WCSP, 2022).

56 The high number of species and complex patterns of morphological variation has presented  
57 significant challenges for resolving relationships in *Bulbophyllum* and this is reflected in substantial  
58 taxonomic revisions that have been proposed. Traditionally, the subtribe Bulbophyllinae Schltr. (tribe  
59 Dendrobieae Endl.) included the large genus *Bulbophyllum* along with smaller genera, such as  
60 *Cirrhopetalum* Lindl., *Drymoda* Lindl., *Pedilochilus* Schltr., *Sunipia* Buch.-Ham. ex Sm., and *Trias*  
61 Lindl. (Dressler, 1993; Garay et al., 1994; Szlachetko and Margonska, 2001). Recent revisions treat  
62 all genera within the subtribe Bulbophyllinae in a more broadly defined *Bulbophyllum* and recognise  
63 97 sections within the genus (Pridgeon et al., 2014; Vermeulen et al., 2014). Molecular phylogenetic  
64 studies have largely focused on species from specific geographic regions such as Madagascar and the  
65 Mascarenes (Fischer et al., 2007; Gamisch et al., 2015), the Neotropics (Smidt et al., 2013, 2011),  
66 and Peninsular Malaysia (Hosseini et al., 2012) or on taxonomic groups such as the *Cirrhopetalum*  
67 alliance (Hu et al., 2020), and few have taken a global perspective (e.g., Gamisch and Comes, 2019).  
68 These studies revealed a strong biogeographic pattern within the genus with four main clades that  
69 include species largely confined or endemic within one broader geographical area: 1) continental  
70 Africa, 2) Madagascar and the Mascarene Islands, 3) Southern America, or 4) Asia (Fischer et al.,  
71 2007; Gamisch et al., 2015; Gamisch and Comes, 2019; Smidt et al., 2011). The Southern American  
72 clade, the Madagascan clade, and the continental African clade together form a highly supported  
73 lineage (Fischer et al., 2007; Gamisch et al., 2015; Gamisch and Comes, 2019; Smidt et al., 2013;  
74 2011), in sister group position to the Asian clade (Fischer et al., 2007; Gamisch et al., 2015; Gamisch  
75 and Comes, 2019). Previous molecular phylogenetic studies have mainly elucidated relationships  
76 within Madagascan, continental African and Neotropical sections and within the *Cirrhopetalum*  
77 alliance (Fischer et al., 2007; Gamisch et al., 2015; Smidt et al., 2011; Hu et al., 2020). However,  
78 evolutionary relationships within the Asian clade, which also includes taxa from the Australasian and  
79 Pacific regions, are still poorly understood, and the monophyly of sections within this clade has  
80 remained largely untested within a phylogenetic framework.

81

82 The study of hyper diverse groups such as *Bulbophyllum* requires a robust phylogenetic framework to  
83 assess monophyly of its infrageneric taxa. High throughput sequencing approaches facilitate the

84 establishment of such a framework phylogeny to clarify broader evolutionary relationships and to  
85 assess the monophyly of infrageneric taxa and their trait evolution (Hassemer et al., 2019; van  
86 Kleinwee et al., 2022, Nargar et al. 2022). However, phylogenomic studies which provide insights  
87 into broad-level evolutionary relationships within the Asian clade of *Bulbophyllum* are still lacking.  
88 This hampers progress in understanding diversification of its evolutionary lineages in time and space  
89 and trait evolution within this highly diverse genus.

90 Within *Bulbophyllum*, section *Adelopetalum* has a unique distribution, being the only section with a  
91 centre of diversity in Australia (Brummit, 2001; Pridgeon et al., 2014, Vermeulen, 1993), and thus  
92 presents an interesting study case for range evolution within *Bulbophyllum*. The section comprises  
93 twelve tropical to temperate epi-lithophytic species. Nine species occur along Australia's east coast  
94 in the montane forest communities of the Great Dividing Range, with one species (*B. argyropus*) also  
95 found on Australian islands (Lord Howe Island, and Norfolk Island). Two species are endemic to the  
96 montane forests of New Caledonia (*B. corythium*, *B. lingulatum*) and one to the lowland coastal  
97 forests of New Zealand (*B. tuberculatum*). The section was circumscribed based on morphological  
98 affinities recognised among ten species from Australia and New Caledonia previously assigned to  
99 *Bulbophyllum* sections *Desmosanthes*, *Racemosae* and *Sestochilus* (Dockrill, 1969; 1992;  
100 Vermeulen, 1993). Subsequent treatments recognised two additional species within the section, *B.*  
101 *weinthalii* and *B. exiguum* (Jones and Clements, 2002; Clements and Jones, 2006). Section  
102 *Adelopetalum* is characterised by plants having thin creeping rhizomes adpressed to the host,  
103 anchored by filamentous roots with small pseudobulbs that are crowded to widely spaced, and a  
104 small single flat leaf arising from the apex of the pseudobulb. The inflorescence is single to few-  
105 flowered, with small white, cream or yellow flowers, sometimes with red or purple patterns. The  
106 petals are smaller than the sepals but similar in shape, with the bases of the lateral sepals fused to the  
107 column foot. The fleshy three-lobed labellum is firmly hinged to the apex of the column foot.

108 Previous cladistic analysis of sect. *Adelopetalum* based on morphological characters resolved two  
109 main clades within the section, differentiated by the size and shape of the lower margin of the  
110 stelidia: the filiform column appendages typical for most *Bulbophyllum* (Vermeulen, 1993). Previous  
111 molecular phylogenetic studies based on the nuclear ribosomal ITS region (ITS1 + 5.8S + ITS2)  
112 included two to three representatives of the section (Gamisch et al., 2015; Gamisch and Comes,  
113 2019), placing these in an early diverging position within the Asian clade. However, phylogenetic  
114 placement of the section within *Bulbophyllum* was not strongly supported (PP<90, BS 97) and thus  
115 requires further study. Further, phylogenetic relationships within sect. *Adelopetalum* and its ancestral  
116 range evolution are poorly understood and have not yet been investigated using a molecular  
117 phylogenetic approach.

118 The aims of this study were to 1) build a phylogenomic framework for *Bulbophyllum* with focus on  
119 the Asian clade 2) assess the monophyly and phylogenetic placement of sect. *Adelopetalum* within  
120 *Bulbophyllum*; 3) to infer interspecific relationships within sect. *Adelopetalum* 4) and to reconstruct  
121 the range evolution of sect. *Adelopetalum*.

## 122 **2 Materials and methods**

### 123 **2.1 Sampling**

124 In total, 136 orchid samples representing 114 species were included in the study. From the Asian,  
125 Australasian and Pacific regions a broad sampling was included representing 41 sections, i.e. 60% of  
126 sections recognised from these regions in the most recent treatment of the group (Pridgeon et al.,  
127 2014). From the Australasian region, all *Bulbophyllum* species were sampled (Australia: 30, New

128 Zealand: 2). For *Bulbophyllum* sect. *Adelopetalum*, 28 samples were included, representing all 12  
129 species recognised for the section. The morphologically closely related sect. *Minutissima* was  
130 included with nine samples representing five species comprising all four Australasian and Pacific  
131 species and two (of ca. 19) tropical Asian species. Sampling of representative species for the  
132 Afrotropical and Neotropical clades of *Bulbophyllum* was informed by previous phylogenetic studies  
133 (Fischer et al., 2007; Smidt et al., 2011; Gamisch and Comes, 2019). Species names follow the  
134 accepted taxonomy based on the World Checklist of Selected Plant Families (WCSP, 2022) and  
135 sectional taxonomy IOSPE (2022). Exceptions were made for *B. exiguum* which was placed in  
136 section *Adelopetalum* and *B. wolfei* which was placed in section *Polymeres* based on Jones and  
137 Clements (2002) and Clements and Jones (2006). The outgroup comprised representatives of subtribe  
138 Dendrobineae which is sister to Bulbophyllinae, and tribes Malaxideae, Arethuseae, Nervilleae, and  
139 Neottieae based on previous molecular phylogenetic studies (Givnish et al., 2015; Górniak et al.,  
140 2010, Serna-Sánchez et al. 2021). Details of the plant material studied, voucher information and the  
141 number of loci included for each sample are provided in Supplementary Material S1 and a complete  
142 list of loci analysed is provided in Supplementary Material S2.

## 143 2.2 DNA extraction, amplification, and sequencing

144 Total genomic DNA was extracted from ca. 10 to 20 mg silica-dried leaf material. Extractions were  
145 carried out with commercial extraction kits (Qiagen DNeasy plant kit, Venlo, Netherlands;  
146 ChargeSwitch gDNA plant kit, Invitrogen, Carlsbad, USA) following the manufacturer's protocols or  
147 using the CTAB method (Doyle and Doyle, 1990), with modifications as described in Weising et al.  
148 (2005). Sequence data was generated using both Sanger sequencing (46 samples) for the nuclear  
149 ribosomal ITS region (ITS1, 5.8s, ITS2) and two plastid genes (*matK*, *ycf1*) and shotgun high-  
150 throughput sequencing (89 samples) to extract 70 plastid coding sequences (CDS) and the nuclear  
151 ribosomal DNA cistron (Supplementary Material S2) for subsequent analyses. Libraries for high-  
152 throughput sequencing were constructed from 50 to 100 ng total DNA using the TruSeq Nano DNA  
153 LT library preparation kit (Illumina, San Diego, USA) for an insert size of 350 base pairs (bp) and  
154 paired-end reads following the manufacturer's protocol. Libraries were multiplexed 96 times and  
155 DNA sequencing with 125 bp paired-end reads was carried out on an Illumina HiSeq 2500 platform  
156 at the Australian Genomic Research Facility, Melbourne (Australia).

157 For Sanger sequencing, amplifications for ITS were carried out with primers 17F and 26SER (Sun et  
158 al., 1994), for *matK* with the primers 19F and 1326R (Cuénoud et al., 2002), and for *ycf1* with  
159 primers 3720F, intR, intF, 5500R (Neubig et al., 2008). PCR reaction protocols are provided in  
160 Supplementary Material S3. Sequencing reactions were carried out using the amplification primers  
161 and sequencing was conducted on an AB3730xl 96-capillary sequencer (Australian Genome  
162 Research Facility, Brisbane, Australia).

## 163 2.3 Assembly and alignment

164 Sequences were assembled and edited in Geneious R10 (Kearse et al., 2012). Illumina sequences  
165 were assembled to a reference set of plastid CDS extracted from *Dendrobium catenatum* (GenBank  
166 accession numbers KJ862886) and for *ycf68* from *Anoectochilus roxburghii* (KP776980). To build a  
167 reference for the nuclear ribosomal ITS-ETS region, Illumina reads of *B. boonjee* (CNS\_G07175)  
168 were first mapped to the ITS-ETS region of *Corallorhiza trifida* (JVF2676a). To extend the region  
169 assembled, the *B. boonjee* Illumina reads were then mapped to the *B. boonjee* consensus sequence  
170 generated in the initial step, yielding a *B. boonjee* reference of the nuclear ribosomal DNA cistron  
171 (5'ETS, 18s, ITS1, 5.8s, ITS2, 28s, 3'ETS). Illumina sequences for all other samples were assembled  
172 against the *B. boonjee* nuclear ribosomal DNA cistron reference. Assemblies were carried out with

173 the highest quality threshold and a minimum coverage of ten reads. The quality of the assemblies was  
174 checked and edited manually where required. Sequences were deposited in GenBank and ENA. For  
175 Sanger sequences, bidirectional reads were assembled in Geneious and edited manually. Additional  
176 sequences were sourced from DRYAD (<https://doi.org/10.5061/dryad.n9r58>) for *Coelogyne flaccida*  
177 (Givnish et al., 2015). DNA sequences were aligned using MAFFT v.7.222 (Katoh et al., 2005, 2002)  
178 with the default settings, visually inspected and then concatenated into a nuclear and plastid  
179 supermatrix, respectively. The nuclear supermatrix included 136 accessions, partitioned into coding  
180 and non-coding regions (alignment length: 6,341bp, number of parsimony informative sites: 995  
181 (16%)); and the plastid supermatrix included 130 accessions, and 70 plastid coding regions,  
182 partitioned by gene and codon position (alignment length: 61,553bp, number of parsimony  
183 informative sites: 5,789 (9%)). A plastid dataset comprised of high throughput sequencing data only  
184 (excluding Sanger sequences) was produced including 90 accessions, and 70 plastid coding regions  
185 (alignment length: 61,553bp, number of parsimony informative sites: 5682 (9%) and analysed  
186 separately.

187 For divergence time estimations, the plastid supermatrix was reduced to one representative per  
188 species (indicated by an asterisk in Supplementary Material S1), comprising 111 accessions  
189 (alignment length: 60,984 bp, number of parsimony informative sites: 5,755 (9%)).

## 190 **2.4 Phylogenetic analysis**

191 Phylogenetic relationships were inferred using maximum likelihood (ML) in IQ-TREE v. 1.6.12  
192 (Nguyen et al., 2015). The best-fit partition scheme and nucleotide substitution model for each  
193 partition was determined with IQ-TREE's ModelFinder (Kalyaanamoorthy et al. 2017) based on the  
194 Akaike information criterion (AIC) (Akaike, 1974). Nodal support was assessed based on 1000  
195 replicates of ultrafast bootstrap approximation with clades receiving >95 ultrafast bootstrap support  
196 (UFBS) considered as well supported (Minh et al., 2013; Hoang et al., 2018).

## 197 **2.5 Divergence time estimation**

198 Divergence times were estimated based on the plastid dataset in Beast2 v. 2.4.8 (Bouckaert et al.,  
199 2014) applying the best fit partition scheme and substitution model as determined by IQ-TREE's  
200 ModelFinder. We tested two molecular clock models: 1) strict clock (Zuckerandl and Pauling,  
201 1965) and 2) relaxed lognormal clock (Drummond et al., 2006) and two models of speciation and  
202 extinction: 1) Yule and 2) birth-death (Yule, 1925; Gernhard et al., 2008). Three secondary  
203 calibration points were used applying priors with a normal distribution and mean ages and 95%  
204 higher posterior density (HDP) intervals based on the results of a family-wide molecular clock  
205 analysis by Chomicki et al. (2015). The root age was set to 55.02 Ma (HDP: 42.0–68.0). The next  
206 secondary calibration point was applied to the last common ancestor of Dendrobineae, Malaxideae,  
207 and Arethuseae and was set to 47.77 Ma (HDP: 36.4–59.1). Monophyly was constrained for this  
208 node consistent with relationships reconstructed in previous phylogenetic analyses (Chomicki et al.  
209 2015; Givnish et al., 2015). The last secondary calibration was set at the stem node of Dendrobieae  
210 and Malaxideae with 38.68 Ma (HDP: 30.8–46.6). An additional calibration based on the fossil  
211 *Dendrobium winikaphyllum* (Conran et al., 2009) was applied to the stem node of the Australasian  
212 *Dendrobium* clade (*D. macropus*, *D. cunninghamii*, and *D. muricatum*), using a uniform distribution  
213 with an infinite maximum age and the minimum age constrained to 20.4 Ma, based on the minimum  
214 age of the strata containing the fossil (Mildenhall et al. 2014). Ten independent Beast analyses were  
215 run for 30 million MCMC generations, with trees sampled every  $3 \times 10^4$  generations. To assess  
216 convergence of independent runs and determine burn-in fractions, log files were assessed in Tracer  
217 v.1.7.1 (Rambaut and Drummond, 2007). Log and trees files from independent runs were combined

218 in LogCombiner (from the Beast package) with a cumulative burn-in fraction of 10%-31% and the  
219 sampling frequency set to generate at least 10,000 tree and log files (Drummond and Bouckaert,  
220 2015). The combined log file was assessed in Tracer to ensure the effective sample size of all  
221 parameters was above 200. An additional five independent Beast runs were conducted for the final  
222 analysis using a relaxed log normal clock with birth death speciation to achieve an effective sample  
223 size above 200 for the uclmean parameter. A maximum clade credibility tree was generated in  
224 TreeAnnotator (Beast package) with median node heights. To compare clock and speciation models,  
225 the Akaike information criterion by MCMC app from the BEAST 2 package v 2.6.2 was used to  
226 measure the AICM for the combined MCMC runs generated in the BEAST analysis for each model  
227 (Supplementary Material S4).

## 228 **2.6 Ancestral range analysis**

229 Species distributions were extracted from WCSP (2022). Biogeographic areas were largely  
230 delineated based on botanical continents defined by Brummit (2001). The subcontinental regions of  
231 Papuasia, Australia and New Zealand were recognised to allow a more fine-scaled resolution of range  
232 evolution in section *Adelopetalum* (Brummit 2001). The following seven biogeographic areas were  
233 coded: a, Africa; b, temperate Asia; c, tropical Asia; d, Papuasia; e, Australia; f, New Zealand, and g,  
234 Pacific. Ancestral ranges were estimated in RASP v. 4.0 (Yu et al., 2015) with the BioGeoBEARS  
235 package (Matzke, 2013) based on the maximum clade credibility tree obtained from the Beast  
236 analysis of the plastid supermatrix, pruned of the outgroups to Dendrobieae. Three models of range  
237 evolution were tested: the dispersal-extinction cladogenesis model (DEC) (Ree and Smith, 2008), a  
238 ML version of Ronquist's parsimony dispersal-vicariance (DIVA; Ronquist, 1997), termed  
239 DIVALIKE (Matzke, 2013), and a simplified likelihood interpretation of the Bayesian "BayArea"  
240 program (Landis et al., 2013) known as BAYAREALIKE (Matzke, 2013). No constraints were  
241 applied to dispersal direction and the maximum number of ranges was set to five based on the  
242 maximum number of observed areas in extant species. Likelihood values were compared and the  
243 model of best fit determined by AIC score (Akaike, 1974) was used to infer the marginal  
244 probabilities of alternative ancestral ranges at each node in the phylogeny (Supplementary Material  
245 S5).

## 246 **3 Results**

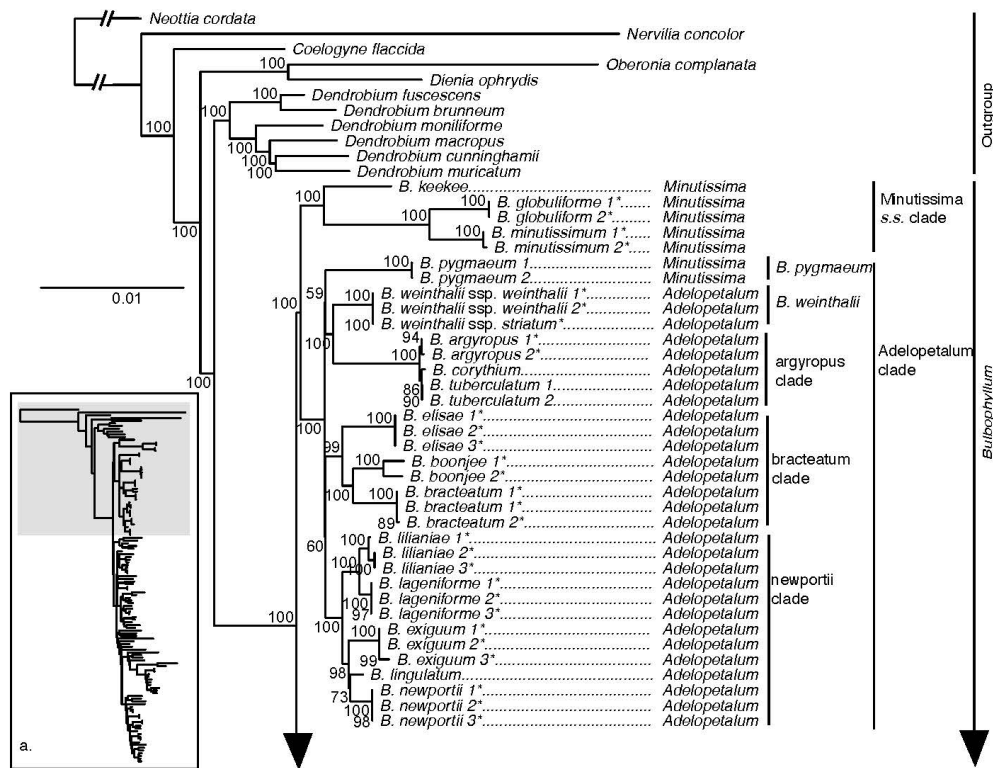
### 247 **3.1 Phylogenetic relationships**

#### 248 **3.1.1 Phylogenetic relationships – Plastid data**

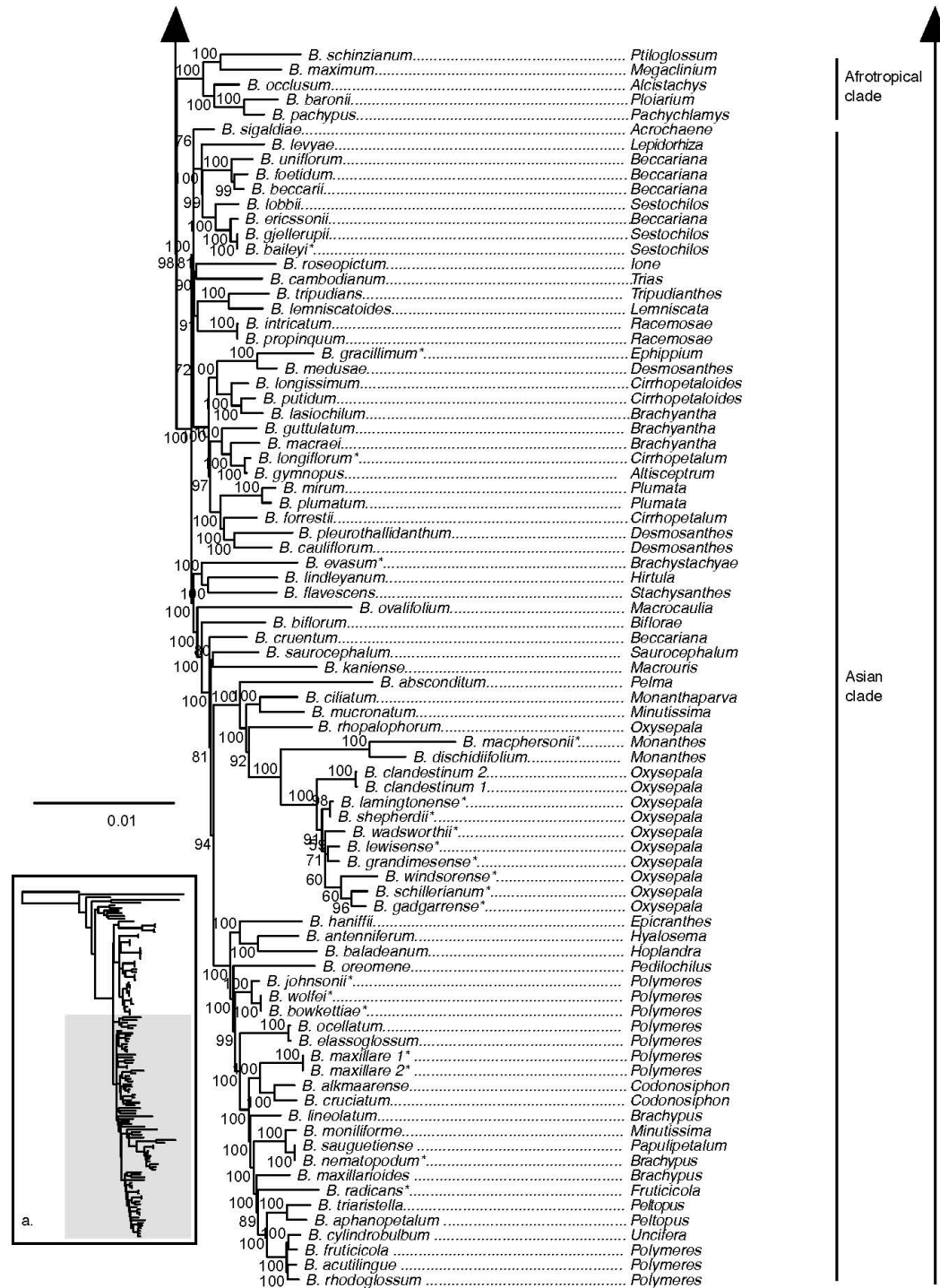
249 The ML phylogeny inferred from the 70 loci plastid supermatrix provided strong support for the  
250 monophyly of *Bulbophyllum* and its sister group relationship to *Dendrobium* (Fig. 1). Section  
251 *Adelopetalum* and *Minutissima s.s.* formed a highly supported clade, here termed the  
252 *Adelopetalum/Minutissima* clade, which was resolved in sister group position to the remainder of the  
253 genus (ultrafast bootstrap support/UFBS 98) (Fig. 1, Fig. 2). Within the *Adelopetalum/Minutissima*  
254 clade, all *Adelopetalum* species plus *B. pygmaeum* (sect. *Minutissima*) formed a highly supported  
255 lineage (UFBS 100), here termed the *Adelopetalum* clade. Within the *Adelopetalum* clade several  
256 highly supported groups were resolved: 1) the argyropus clade consisting of *B. argyropus*, *B.*  
257 *corythium* and *B. tuberculatum* (UFBS 100), reconstructed in a highly supported sister group  
258 relationship to *B. weinthalii* (UFBS 100); 2) the bracteatum clade, including *B. boonjee*, *B.*  
259 *bracteatum*, and *B. elisae* (UFBS 99); and 3) the newportii clade comprised of *B. exiguum*, *B.*  
260 *lageniforme*, *B. lilianae*, *B. lingulatum*, and *B. newportii* (UFBS 100). Relationships among *B.*  
261 *pygmaeum*, the argyropus clade + *B. weinthalii*, bracteatum and newportii clades received weak

262 support. Sister to the Adelopetalum clade was the highly supported Minutissimum clade comprised  
 263 of three species of sect. *Minutissima* (*B. globuliforme*, *B. keekee*, *B. minutissimum*), including the  
 264 type species of the section (UFBS 100) (Fig. 1). Section *Minutissima* was identified as polyphyletic,  
 265 with sect. *Minutissima* species placed within the Adelopetalum clade (*B. pygmaeum*) and the Asian  
 266 clade (*B. mucronatum*, *B. moniliforme*). Within the Asian clade, sections *Beccariana*, *Brachyantha*,  
 267 *Brachypus*, *Cirrhopetaloides*, *Cirrhopetalum*, *Desmosanthes*, *Oxysepala*, *Polymeres* and *Sestochilos*  
 268 were identified as polyphyletic or paraphyletic. Phylogenetic relationships described here based on  
 269 the plastid supermatrix (Fig.1, Fig. 2) are supported by reconstructions based on the 70 gene plastid  
 270 dataset (Supplementary Material S6).

271 Our analyses showed that sect. *Adelopetalum* does not share a close relationship with other  
 272 Australasian *Bulbophyllum* species, such as those in sect. *Brachypus* (*B. nematopodum*), sect.  
 273 *Brachystachyae* (*B. evasum*), sect. *Cirrhopetalum* (*B. longiflorum*), sect. *Ephippium* (*B.*  
 274 *gracillimum*), sect. *Monanthes* (*B. macphersonii*), sect. *Oxysepala* (*B. gadgarrense*, *B.*  
 275 *grandimesense*, *B. lamingtonense*, *B. lewisense*, *B. schillerianum*, *B. shepherdii*, *B. wadsworthii*, *B.*  
 276 *windsorensense*), sect. *Polymeres* (*B. bowkettiae*, *B. johnsonii*, *B. radicans*, *B. wolfei*), and sect.  
 277 *Sestochilus* (*B. baileyi*). Australian species from each of these sections were placed in nine different  
 278 positions within the Asian clade. Australian species from section *Polymeres* formed a highly  
 279 supported clade (UFBS 100), while Australian species from sect. *Oxysepala* formed a moderately  
 280 supported clade (UFBS 91) and together with the type species of section *Oxysepala* from Papuaia  
 281 (*B. cladistinum*) formed a close relationship with the Australian representative of section *Monanthes*  
 282 (*B. macphersonii*) (UFBS 100).



283 Figure 1.  
 284 Maximum likelihood phylogenetic reconstruction of *Bulbophyllum* based on the supermatrix of 70  
 285 plastid coding regions in inset a. with *Bulbophyllum* sections *Adelopetalum* and *Minutissima* s.s. in  
 286 detail. Ultrafast bootstrap values are given adjacent to nodes. Australian species are shown with an  
 287 asterisk.



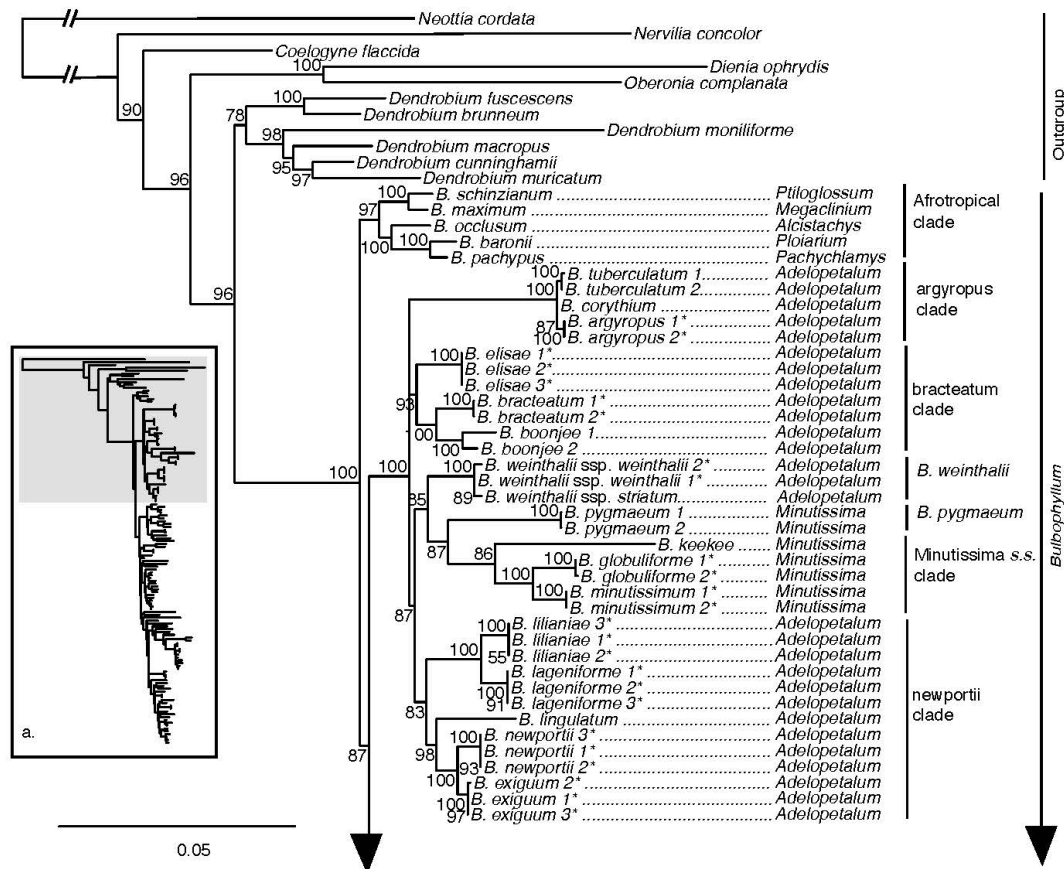
288  
 289 Figure 2. Maximum likelihood phylogenetic reconstruction of *Bulbophyllum* based on the  
 290 supermatrix of 70 plastid coding regions in inset a. with Afrotropical and Asian *Bulbophyllum* clades  
 291 in detail. Ultrafast bootstrap values are given adjacent to nodes. Australian species are shown with an  
 292 asterisk.



### 293 3.1.2 Phylogenetic relationships – Nuclear data

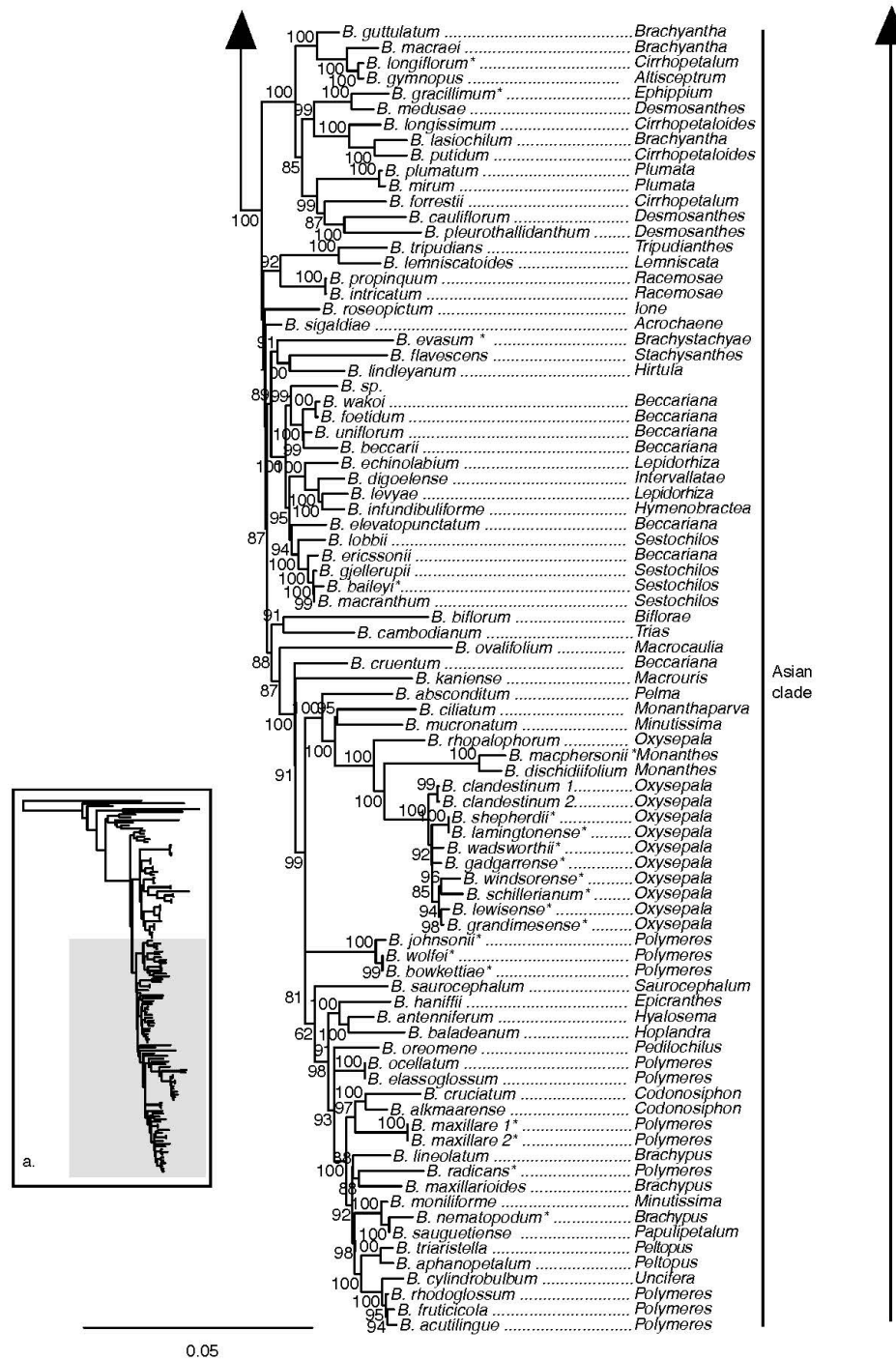
294 The ML phylogeny based on the nuclear ribosomal DNA cistron was resolved with overall lower  
 295 support compared to analyses based on 70 plastid loci supermatrix (Fig. 3, Fig. 4). Relationships  
 296 among outgroup taxa were concordant with the plastid phylogeny and *Bulbophyllum* was resolved  
 297 with maximum support. Within *Bulbophyllum*, the Afrotropical (UFBS 97), Asian (UFBS 100) and  
 298 Adelopetalum/Minutissima (UFBS 100) clades were resolved with high to maximum support,  
 299 however the relationships among them were poorly supported. Within the Adelopetalum/Minutissima  
 300 clade, the highly supported clades revealed in the plastid phylogeny were also reconstructed based on  
 301 the nuclear dataset (argyropus clade (UFBS 100), bracteatum clade (UFBS 93), minutissimum clade  
 302 (UFBS 86), and newportii clade (UFBS 83), however relationships among these remained poorly  
 303 supported. Similar to reconstructions based on the plastid phylogeny were the relationships among  
 304 the argyropus, bracteatum and newportii clades, the poor support of *B. pygmaeum* and *B. weinthalii*,  
 305 the polyphyly or paraphyly for sections *Beccariana*, *Brachyantha*, *Brachypus*, *Cirrhopetaloides*,  
 306 *Cirrhopetalum*, *Desmosanthes*, *Minutissima*, *Oxysepala*, *Polymeres*, and *Sestochilos*; and that  
 307 Australian species from sect. sect. *Brachypus*, sect. *Brachystachyae*, sect. *Cirrhopetalum*, , sect.  
 308 *Ephippium*, sect. *Monanthes*, sect. *Oxysepala*, , sect. *Polymeres*, and sect. *Stenochilus* were placed in  
 309 nine clades across the Asian clade.

310



311

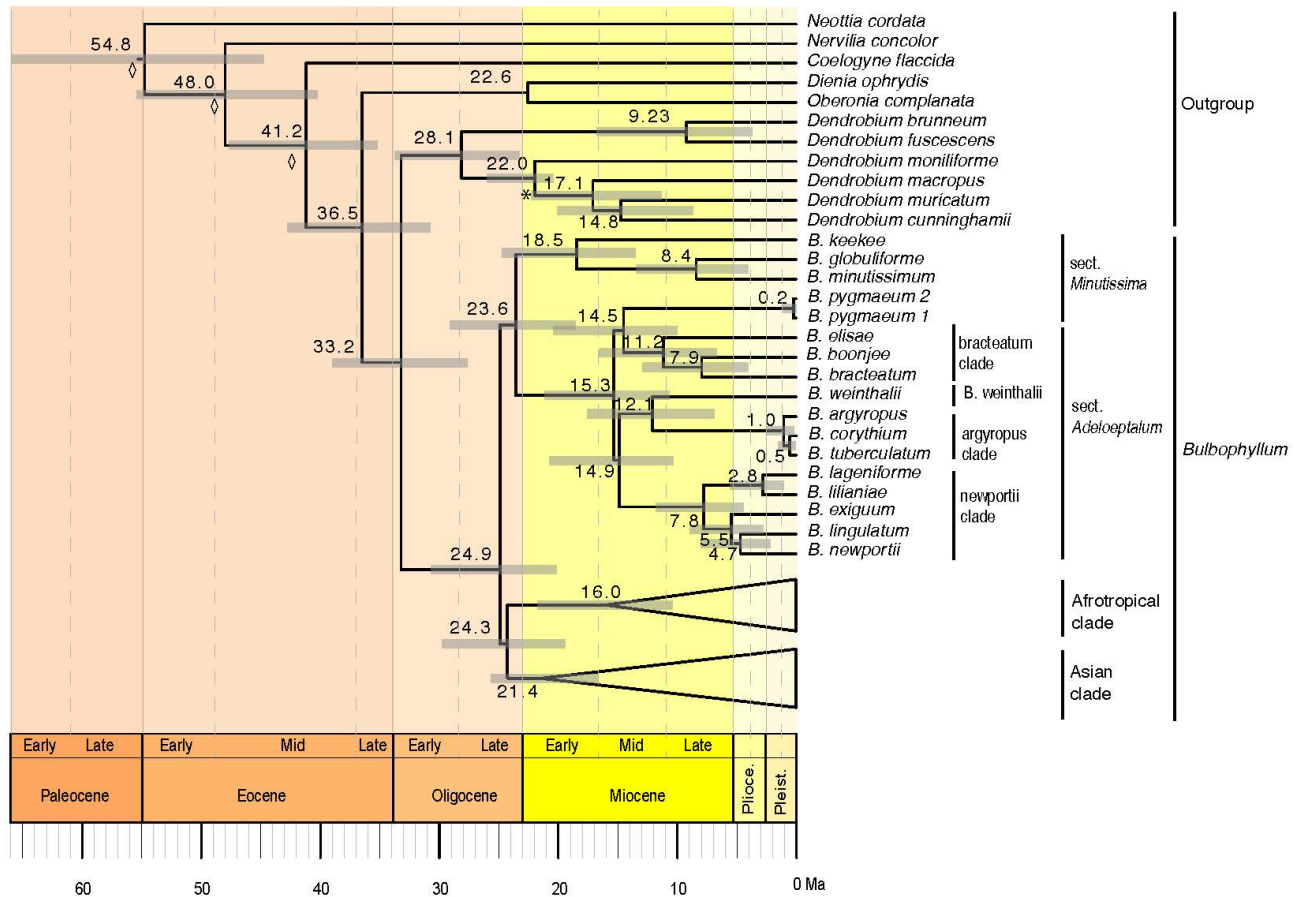
312 Figure 3. Maximum likelihood phylogenetic reconstruction of *Bulbophyllum* based on the nuclear  
 313 ribosomal DNA cistron (5'ETS, 18s, ITS1, 5.8s, ITS2, 28s, 3'ETS) in inset a. with *Bulbophyllum*  
 314 sections *Adelopetalum* and *Minutissima* in detail. Ultrafast bootstrap values are given adjacent to  
 315 nodes. Australian species are shown with an asterisk.



316  
 317 Figure 4. Maximum likelihood phylogenetic reconstruction of *Bulbophyllum* based on nuclear  
 318 ribosomal DNA cistron (5'ETS, 18s, ITS1, 5.8s, ITS2, 28s, 3'ETS) in inset a. with Afrotropical and  
 319 Asian *Bulbophyllum* clades in detail. Ultrafast bootstrap values are given adjacent to nodes.  
 320 Australian species are shown with an asterisk.

### 321 3.2 Divergence time estimation

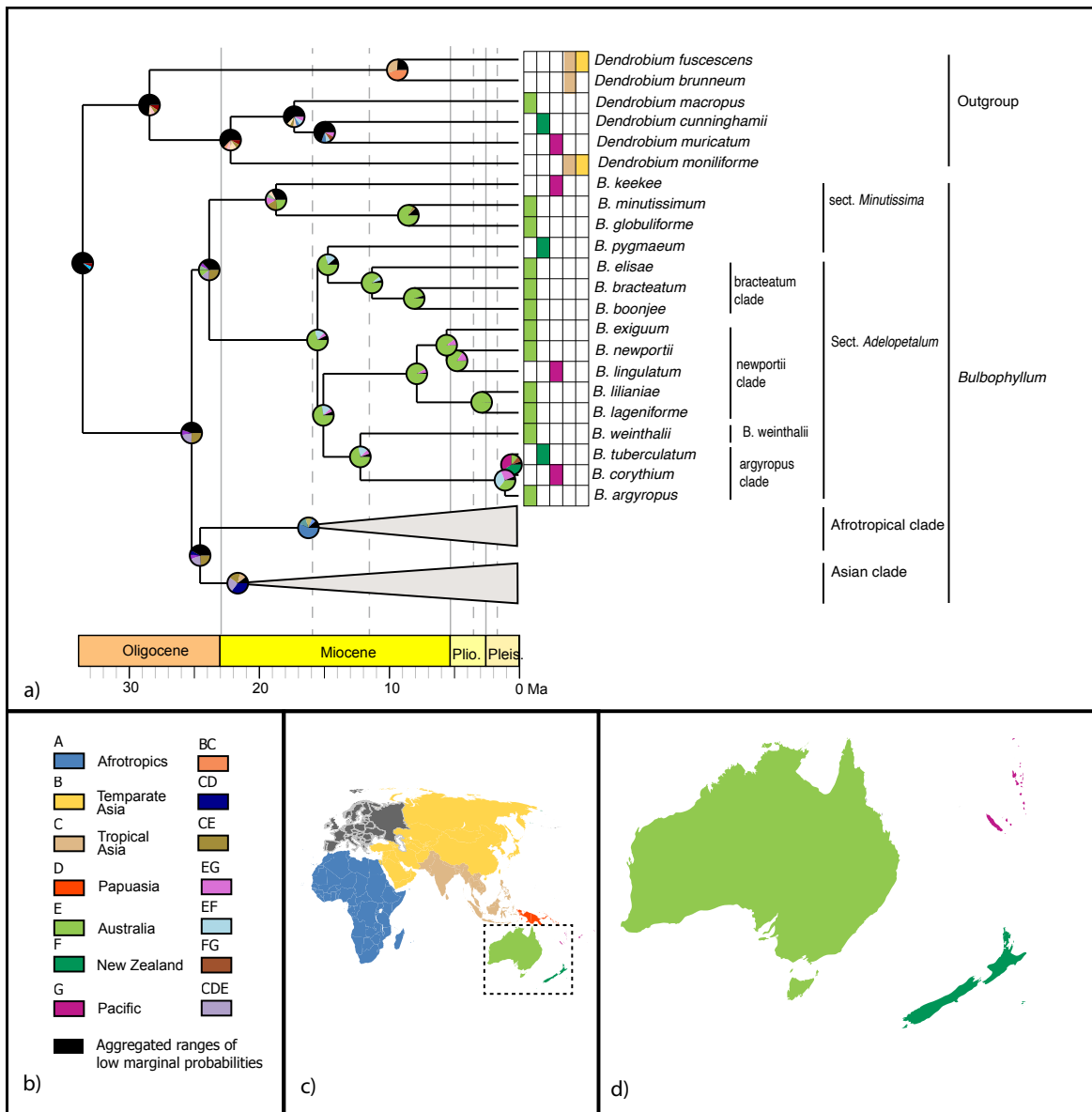
322 The divergence time analysis based on a relaxed log normal clock and birth death prior with  
323 speciation and extinction, which was identified as the model of best fit based on the Akaike  
324 information criterion (Supplementary Material S4), is presented here (Fig. 5) with the Asian and  
325 Afrotropical clades collapsed and the complete chronogram provided in Supplementary Material S7.  
326 The divergence time analysis based on the plastid dataset was well resolved and highly supported  
327 (Fig. 5, Supplementary Material S7). The divergence between *Bulbophyllum* and *Dendrobium* was  
328 estimated to have occurred during the early Oligocene, ca. 33.2 Ma (95% highest posterior  
329 probability density, HPD: 27.7–39.0). The crown of *Bulbophyllum*, constituting the divergence of the  
330 Adelopetalum/Minutissima clade from the remainder of the genus, was dated to the late Oligocene,  
331 ca. 24.9 Ma (HPD: 20.1–30.7). Divergence between the Asian clade and the Afrotropical clade was  
332 estimated to have taken place during the late Oligocene, ca. 24.3 Ma (HPD: 19.4–29.8) and  
333 diversification within the Asian clade was estimated from the mid Miocene 21.4 Ma (HPD: 17.2–  
334 26.4 Ma) and the Afrotropical clade from 16.0 Ma (HPD: 10.4–21.7). The crown age of the  
335 Adelopetalum/Minutissima clade was dated to the late Oligocene, ca. 23.6 Ma (HPD: 18.6–29.1),  
336 with the split of the Minutissimum clade from the Adelopetalum clade. The crown age of the  
337 Adelopetalum clade was dated to the mid Miocene, ca. 15.3 Ma (HPD: 10.6–21.2). The stem  
338 branches of major lineages within the Adelopetalum clade were estimated to have diversified during  
339 the mid-Miocene: the bracteatum clade was dated to ca. 14.5 Ma (HPD: 10.0–20.4); the lineage  
340 giving rise to *B. weinthalii* to ca. 12.1 Ma (6.9–17.6); the argyropus clade to ca. 12.1 Ma (6.9–17.6);  
341 and the newportii clade to ca. 14.9 Ma (HPD 10.3–20.7). Diversification among species within these  
342 lineages took place from the mid-Miocene onwards with the most recent divergence identified during  
343 the late Pleistocene among *B. argyropus*, *B. corythium*, and *B. tuberculatum*.



344  
 345 Figure 5. Maximum clade credibility chronogram for *Bulbophyllum* sect. *Adelopetalum* based on 70  
 346 plastid coding sequences, relaxed log normal clock and birth death prior. Divergence dates and 95%  
 347 highest posterior density values are indicated adjacent to nodes. Grey bars indicate 95% highest  
 348 posterior density. The asterisk denotes the node constrained with a fossil calibration point; the  
 349 diamond shape denotes nodes which were constrained by secondary calibration points.

### 350 3.3 Ancestral range analysis

351 Model testing of the three biogeographic models (DEC, DIVALIKE, BAYAREALIKE) using the  
 352 Akaike information criterion identified the BAYAREALIKE model as the model of best fit for the  
 353 ancestral range estimation (Supplementary Material S5). Ancestral ranges estimated with the  
 354 BAYAREALIKE model are presented here with the Asian and Afrotropical clades collapsed (Fig. 6).  
 355 The complete chronogram is provided in Supplementary Material S8, marginal probabilities for  
 356 ancestral ranges at all nodes in Supplementary Material S9 and node IDs in Supplementary Material  
 357 S10.



358

359 Figure 6. Range evolution of *Bulbophyllum* sect. *Adelopetalum*. a) ancestral area reconstruction based  
 360 on a the BAYAREALIKE model with species extant distributions shown within the grid and pie  
 361 charts at internal nodes representing marginal probabilities for alternative ancestral areas; b) legend  
 362 of color-coded geographic regions and shared ancestral areas; c) world map of color-coded  
 363 geographic regions delineated in the biogeographic analysis; d) detail of Australasian color-coded  
 364 geographic regions.

365 Australia was reconstructed as the most likely ancestral range for the MRCA of the Adelopetalum  
 366 clade (range probability (RP) 82) and all nodes within this lineage (RP 72-99) except for the  
 367 argyropus clade (Fig. 6). Range shifts from Australia were inferred from the early Pliocene to the  
 368 Pacific region (New Caledonia) in the newportii clade, in the lineage giving rise to *B. lingulatum*.  
 369 Range shifts were also inferred from Australia to the Pacific region (New Caledonia) and New  
 370 Zealand either in the lineage giving rise to the MRCA of the argyropus clade or subsequently within  
 371 this lineage. Three alternative ancestral ranges were reconstructed for the MRCA of the argyropus  
 372 clade: Australia (RP 36), or widespread distributions including Australia and New Zealand (RP 33)  
 373 or Australia and New Caledonia (RP 26). Two alternative ranges were also reconstructed for the

374 MRCA of *B. corythium* and *B. tuberculatum*: New Zealand (RP 41) and New Caledonia (RP 34).  
375 Considering these alternative scenarios, range shifts within the argyropus clade were estimated to  
376 have occurred sometime between the mid Miocene and late Pliocene (12.1–0.5 Ma). The ancestral  
377 range of MRCA of the Adelopetalum/Minutissima clade and Bulbophyllum remained unresolved in  
378 the ancestral range reconstruction. The most likely ancestral range for the MRCA of the  
379 Adeloptalum/Minutissima clade was a widespread distribution across Australia and tropical Asia (RP  
380 26), while alternative ranges reconstructed included a widespread range including Australia, tropical  
381 Asia and Papuasia (RP 13) and Australia (RP 11). Two alternative ancestral ranges were  
382 reconstructed for the MRCA of Bulbophyllum, both widespread distributions including Australia and  
383 tropical Asia (RP 25.9) or Australia, tropical Asia and Papuasia (RP 21).

## 384 4 Discussion

### 385 4.1 Phylogenetic relationships

386 This study provided a broad plastid phylogenetic framework for Asian and Australasian sections of  
387 *Bulbophyllum* and revealed a close relationship between sections *Adelopetalum* and *Minutissima s.s.*,  
388 that together form a highly supported early diverging lineage within the genus (Fig. 1, Fig. 2).  
389 Relationships based on 70 plastid genes support a sister group relationship between the  
390 *Adelopetalum/Minutissima* clade and the remainder of the genus (Asian + Afrotropical clades).  
391 Within the *Adelopetalum/Minutissima* clade, analyses based on our 70 plastid loci supermatrix  
392 showed a dichotomous split between the highly supported *Minutissima s.s.* and *Adelopetalum* clades.  
393 Species were reconstructed in each of these clades according to their sectional placement except for  
394 New Zealand endemic *B. pygmaeum* (sect. *Minutissima*), which was nested within the *Adelopetalum*  
395 clade, rendering section *Adelopetalum* paraphyletic. Section *Minutissima* was identified as  
396 polyphyletic, with the Australian (*B. minutissimum* (sect. type), *B. globuliforme*) and Pacific species  
397 (*B. keekee*) placed in the *Minutissima* clade and New Zealand species (*B. pygmaeum*) in the  
398 *Adelopetalum* clade while the Asian species, *B. mucronatum* and *B. moniliforme* were resolved  
399 within the Asian clade. Section *Minutissima* has undergone numerous taxonomic changes with  
400 treatments ranging from a narrower circumscription recognising species from Australia (Jones and  
401 Clements, 2001), to broader classifications including 23 species from Thailand, Indonesia, Australia,  
402 New Zealand, New Caledonia, and New Guinea (Pridgeon et al. 2014). Our phylogenetic analysis  
403 based on plastid and nuclear markers did not reconstruct a close relationship between sect.  
404 *Minutissima* species from the Australasian/Pacific region and Asian species *B. mucronatum* and *B.*  
405 *moniliforme*. Rather, in our analyses the Australasian species fell within the  
406 *Adelopetalum/Minutissima* clade while the Asian species were nested within the Asian clade. The  
407 results support morphological studies differentiating sect. *Minutissima* species from Australasia and  
408 Asia (Jones and Clements, 2001) and show minute pseudobulbs are a trait that has evolved more than  
409 once independently in the genus.

410 Within section *Adelopetalum*, phylogenetic analyses supported current species concepts, except for  
411 species within the argyropus clade, which exhibited shallow genetic differentiation (Fig. 1, Fig. 3).  
412 The species of the argyropus clade share morphological affinities and previous taxonomic treatments  
413 recognised up to three species within the group: *B. argyropus* (Australia's east coast and off shore  
414 islands: Lord Howe Island, and Norfolk Island), *B. corythium* (New Caledonia), and *B. tuberculatum*  
415 (New Zealand) (Clements and Jones, 2002; Halle, 1981; Vermeulen, 1993). Divergence dating  
416 analyses shows this group represents a relatively recent radiation reconstructing divergence among  
417 species during the Pleistocene. Further studies are required to clarify species delimitation and  
418 dispersal patterns utilising population-level sampling and genomic techniques suited to resolving

419 relationships among recently diverged lineages, such as reduced representation high-throughput  
420 approaches like ddRAD, DArT or target sequence capture methods (Peterson et al., 2012; Sansaloni  
421 et al., 2011; Weitemier et al., 2014; Folk et al., 2015; Bagley et al. 2020, Schmidt-Lebuhn et al.,  
422 2022).

423 Previous cladistic analysis based on morphological traits in sect. *Adelopetalum* found two main  
424 clades within the section, one comprising *B. lageniforme*, *B. lilianae*, *B. lingulatum*, and *B.*  
425 *newportii*, and the other uniting *B. argyropus*, *B. bracteatum*, and *B. elisae* (Vermeulen 1993).  
426 Phylogenetic relationships based on plastid and nuclear markers found strong to moderate support for  
427 the first clade recovered in the cladistic analysis, corresponding to the *newportii* clade in the present  
428 analyses (Fig 1, Fig. 3). The second group found in the cladistics analysis included three species  
429 placed in phylogenetic analyses within either the *bracteatum* clade (*B. bracteatum*, *B. elisae*) or the  
430 *argyropus* clade (*B. argyropus*). However, relationships among these two lineages remained unclear  
431 due to low support. The sister group relationship between *B. bracteatum* and *B. argyropus* recovered  
432 in the cladistic analysis was not supported in phylogenetic reconstructions based on molecular data,  
433 suggesting character states shared by these species may be homoplasious. Further studies using  
434 ancestral character reconstruction are required to test the phylogenetic utility of morphological traits  
435 utilised in prior studies.

436 While plastid phylogenomics has clarified major clades and intraspecific relationships within sect.  
437 *Adelopetalum* and broad-level relationships within *Bulbophyllum*, further studies are required. Non-  
438 monophyletic sections identified in the present study (e.g., sections *Beccariana*, *Brachyantha*,  
439 *Brachypus*, *Cirrhopetaloides*, *Cirrhopetalum*, *Desmosanthes*, *Minutissima* and *Polymeres*) (Fig. 2)  
440 and in previous molecular phylogenetic studies (Fischer et al., 2007; Smidt et al., 2011; Pridgeon et  
441 al. 2014; Hu 2020) highlight the need for further taxonomic revision within *Bulbophyllum*. Studies  
442 are required with an expanded sampling of the diverse Asian and Pacific taxa to increase our  
443 understanding of evolutionary relationships and assess sectional classification in more detail.  
444 Phylogenetic relationships reconstructed from the nuclear ribosomal DNA cistron were not strongly  
445 supported in line with previous molecular studies based in ITS (Gamisch et al., 2015; Gamisch and  
446 Comes, 2019, Hu et al., 2020). Approaches yielding higher number of nuclear markers such as target  
447 sequence capture, provide an opportunity to improve the understanding of evolutionary relationships  
448 in future studies. While assembling datasets with comprehensive species coverage within mega  
449 diverse groups such as *Bulbophyllum* remains a challenge, the present study provides an example of  
450 the use of a broad phylogenetic framework with targeted sampling within a section, to test the  
451 monophyly and phylogenetic placement of groups of interest.

## 452 4.2 Spatio-temporal evolution of *Bulbophyllum* sect. *Adelopetalum*

453 Our divergence time analysis and ancestral range estimations showed that *Bulbophyllum* sect.  
454 *Adelopetalum* represents an Australasian lineage that originated on the Australian continent during  
455 the late Oligocene to early Miocene (Fig. 5, Fig. 6). The Australian ancestral range is largely  
456 conserved within the lineage, indicating diversification among species has predominantly taken place  
457 on the Australian continent. The conservation of ancestral range observed within sect. *Adelopetalum*  
458 is consistent with previous phylogenetic analyses of *Bulbophyllum* that have shown a strong  
459 biogeographic signal among clades, being largely confined to biogeographic regions such as  
460 Madagascar, continental Africa and South America (Fischer et al., 2007; Gamisch et al., 2015;  
461 Gamisch and Comes, 2019; Smidt et al., 2011). The evolution of *Bulbophyllum* during the early  
462 Oligocene occurred subsequently to the breakup of Gondwana (Matthews, et al. 2016; Zahirovic et  
463 al. 2016), implicating long-distance dispersal (LDD) in the evolution of biogeographical lineages

464 within the genus (Van den Berg, 2003, Smidt et al., 2011; Gamisch et al., 2015; Gamisch and Comes,  
465 2019). Nevertheless, the conservation of ancestral ranges observed within the *Adelopetalum* lineage  
466 in this study and strong biogeographic signal among clades identified in previous studies indicate  
467 LDD with successful establishment and persistence has been relatively infrequent within  
468 *Bulbophyllum*. Although the minute wind-dispersed seeds of orchids have a high dispersal potential,  
469 successful establishment in a new area are limited by several factors, such as the presence of  
470 mycorrhizal partners necessary for germination and development, a suitable host or substrate and  
471 microclimatic conditions, and the availability of pollinators (Arditti and Ghani, 2000; Jersáková and  
472 Malinová, 2007; McCormick et al., 2012). Our results are consistent with previous studies that have  
473 identified in situ diversification as the dominant biogeographic process, despite evidence for LDD,  
474 and provide further support for the hypothesis that the complex requirements for successful  
475 establishment, rather than dispersal limitations, play an important role in constraining the geographic  
476 distribution of orchids (Givnish et al., 2016; Perez-Escobar and Chomicki et al. 2017).

477

478 Our phylogenetic analysis further resolved interspecific relationships in sect. *Adelopetalum* (Fig. 1).  
479 Divergence time estimation showed that divergence among species occurred mainly during the  
480 Miocene and Pliocene (Fig. 5), during a period of extensive changes to the distribution of forest  
481 vegetation on the Australian continent in response to drastic climatic changes. During the early  
482 Miocene, Australian vegetation diversified in response to aridification of the Australian continent and  
483 the abrupt shift to a cool dry climate during the mid-Miocene resulted in considerable fragmentation  
484 of rainforest habitats (Martin, 2006, Byrne et al. 2011). *Bulbophyllum* sect. *Adelopetalum* comprises  
485 epiphytic species that occur in mesic forest habitats and thus diversification and fragmentation of  
486 these habitats were likely drivers of allopatric lineage divergence within this group. Sister group  
487 relationships were identified between two species pairs with disjunct distributions in Australia's  
488 northern wet tropical rainforests and south-eastern rainforests (*B. boonjee*/*B. bracteatum* and *B.*  
489 *newportii*/*B. exiguum*). These relationships support the hypothesis that the diversification and  
490 fragmentation of forest habitats in Australia has been an important driver of lineage divergence in  
491 Australia's mesic biome (Byrne et al., 2011, Simpson et al., 2018).

492 Whilst the ancestral range was predominantly conserved within the *Adelopetalum* lineage, range  
493 expansion events were inferred from continental Australia across the Coral and Tasman Seas to New  
494 Caledonia in the lineage giving rise to *B. lingulatum*, and to New Zealand and New Caledonia in the  
495 argyropus clade (Fig. 6). New Caledonia and New Zealand each have a long history of isolation from  
496 Australia that predates the evolution of *Bulbophyllum*, indicating colonisation of these islands by  
497 *Bulbophyllum* species has been via LDD (Matthews et al., 2016). It remains unclear if LDD to New  
498 Zealand and New Caledonia in the argyropus clade occurred from the early Miocene in the lineage  
499 giving rise to the MRCA of the group or subsequently within this clade during the late Pleistocene,  
500 thus the spatio temporal evolution of this lineage requires further study.

501 The pattern of eastward dispersal observed in range shifts from Australia, across the Coral and  
502 Tasman Seas, is consistent with dispersal patterns inferred in other angiosperms, including  
503 *Abrotanella*, *Dendrobium*, *Dracophyllum*, *Hebe*, *Korthalsella*, *Leucopogon*, *Northofagus*, *Oreobolus*,  
504 *Pterostylis*, *Rytidosperma* (Chacón et al., 2006; Lavarack et al., 2000; Linder, 1999; Molvray et al.,  
505 1999; Swenson et al., 2001; Puente-Lelièvre et al., 2013; Wagstaff et al., 2010, 2006, 2002, Nargar et  
506 al. 2022). The bias towards eastward dispersal observed within section *Adelopetalum* among other  
507 plant groups may be facilitated by the predominant westerly winds occurring in the southern



508 hemisphere that initiated after the rifting of Australia and South America from Antarctica during the  
509 Eocene (Sanmartín et al., 2007).

### 510 **4.3 Conclusions**

511 This study provided an important phylogenomic framework for the mega genus *Bulbophyllum*  
512 facilitating studies into trait and range evolution within the genus. Several Asian sections were  
513 resolved as paraphyletic warranting taxonomic revisions. Our plastid phylogenomic analyses  
514 revealed an early-diverging lineage within *Bulbophyllum*, composed of sect. *Adelopetalum* and sect.  
515 *Minutissima s.s.* For *Bulbophyllum* sect. *Adelopetalum*, this study reconstructed an origin in the early  
516 Oligocene and identified the Australian continent as ancestral range. Species diversification within  
517 the section occurred predominantly on the Australian continent with fragmentation of mesic habitats  
518 during the Miocene identified as likely drivers of allopatric lineage divergence. Multiple independent  
519 long distance dispersal events were inferred from the Australian continent eastward to the islands of  
520 New Zealand and New Caledonia.

### 521 **5 Conflict of Interest**

522 The authors declare that the research was conducted in the absence of any commercial or financial  
523 relationships that could be construed as a potential conflict of interest.

### 524 **6 Author Contributions**

525 Conceptualization: LS, KN, MAC; Data curation: LS, MAC; Formal Analysis: LS, HKO; Funding  
526 acquisition: LS, KN, DMC, MAC; Investigation and Methodology: LS; Supervision: KN, DCM,  
527 MAC; Writing – original draft: LS; Writing – review and editing: KN, HKO, DCM, MAC. All  
528 authors approved of the final version of the manuscript.

### 529 **7 Funding**

530 This work was supported by the Australian Biological Resources Study (BBR 210-34), the Hermon  
531 Slade Foundation (HSF 16-04), and the Australian Orchid Foundation (AOF 320/17; AOF 325.18.).  
532 The authors acknowledge the contribution of Bioplatforms Australia (enabled by NCRIS) in the  
533 generation of data used in this publication.

### 534 **8 Acknowledgments**

535 The authors wish to acknowledge the use of the Next-Generation Sequencing services and facilities  
536 of the Australian Genomic Research Facilities (AGRF). Plant material was collected under kind  
537 permission of the KuKu Nyungkal traditional owners, Queensland Parks and Wildlife (permit  
538 numbers: WISP11258812, WITK11258712. We thank B. Gray, D.L. Jones, G. McCraith, M.T.  
539 Mathieson, B.P. Molloy, L. Roberts, and P.D. Ziesing Michael Harrison for contributing plant  
540 material to the study. We thank Guillaume Chomicki for providing files utilised for secondary  
541 calibration of our divergence dating analyses.

### 542 **9 References**

543 Akaike, H., 1974. A new look at the statistical model identification. IEEE Trans. Automat. Contr. 19,  
544 716–723. doi:10.1109/TAC.1974.1100705

- 545 Arditti, J., Ghani, A.K.A., 2000. Numerical and physical properties of orchid seeds and their  
546 biological implications. *New Phytol.* 145, 367–421. doi:10.1046/j.1469-8137.2000.00587.x
- 547 Bagley, J. C., Uribe-Convers, S., Carlsen, M. M., & Muchhala, N. (2020). Utility of targeted  
548 sequence capture for phylogenomics in rapid, recent angiosperm radiations: Neotropical *Burmeistera*  
549 bellflowers as a case study. *Molecular Phylogenetics and Evolution*, 152, 106769.
- 550 Bouckaert, R., Heled, J., Kühnert, D., Vaughan, T., Wu, C.-H., Xie, D., Suchard, M.A., Rambaut, A.,  
551 Drummond, A.J., 2014. BEAST 2: A software platform for Bayesian evolutionary analysis. *PLoS*  
552 *Comput. Biol.* 10, e1003537. doi:10.1371/journal.pcbi.1003537
- 553 Brummitt, R.K., 2001. World geographical scheme for recording plant distributions, edition 2. *Hunt*  
554 *Institute for Botanical Documentation*, Carnegie Mellon University, Pittsburgh.
- 555 Byrne, M., Steane, D.A., Joseph, L., Yeates, D.K., Jordan, G.J., Crayn, D., Aplin, K., Cantrill, D.J.,  
556 Cook, L.G., Crisp, M.D., Keogh, J.S., Melville, J., Moritz, C., Porch, N., Sniderman, J.M.K.,  
557 Sunnucks, P., 2011. Decline of a biome : evolution, contraction, fragmentation, extinction and  
558 invasion of the Australian mesic zone biota. *J. Biogeogr.* 38, 1–22. doi:10.1111/j.1365-  
559 2699.2011.02535.x
- 560 Chacón, J., Madriñán, S., Chase, M.W., Bruhl, J.J., 2006. Molecular phylogenetics of *Oreobolus*  
561 (Cyperaceae) and the origin and diversification of the American species. *Taxon* 55, 359–366.  
562 doi:10.2307/25065583
- 563 Chomicki, G., Bidel, L.P.R., Ming, F., Coiro, M., Zhang, X., Wang, Y., Baissac, Y., Jay-Allemand,  
564 C., Renner, S.S., 2015. The velamen protects photosynthetic orchid roots against UV-B damage, and  
565 a large dated phylogeny implies multiple gains and losses of this function during the Cenozoic. *New*  
566 *Phytol.* 205, 1330–1341. doi:10.1111/nph.13106
- 567 Conran, J.G., Bannister, J.M., Lee, D.E., 2009. Earliest orchid macrofossils: early Miocene  
568 *Dendrobium* and *Earina* (Orchidaceae: Epidendroideae) from New Zealand. *Am. J. Bot.* 96, 466–74.  
569 doi:10.3732/ajb.0800269
- 570 Cuénoud, P., Savolainen, V., Chatrou, L.W., Powell, M., Grayer, R.J., Chase, M.W., 2002.  
571 Molecular phylogenetics of Caryophyllales based on nuclear 18S rDNA and plastid *rbcL*, *atpB*, and  
572 *matK* DNA sequences. *Am. J. Bot.* 89, 132–44. doi:10.3732/ajb.89.1.132
- 573 Dockrill, A. W. (1969, 1992). *Australian Indigenous Orchids: The epiphytes, the tropical terrestrial*  
574 *species*. Surrey Beatty & Sons.
- 575 Doyle, J.J., Doyle, J.L., 1990. Isolation of plant DNA from fresh tissue. *Focus* 12, 13–15.
- 576 Dressler, R.L., 1993. Phylogeny and classification of the orchid family. Cambridge University Press.
- 577 Drummond, A. J., & Bouckaert, R. R. (2015). *Bayesian evolutionary analysis with BEAST*.  
578 Cambridge University Press.
- 579 Drummond, A.J., Ho, S.Y.W., Phillips, M.J., Rambaut, A., Rambaut, A., 2006. Relaxed  
580 Phylogenetics and dating with confidence. *PLoS Biol.* 4, e88. doi:10.1371/journal.pbio.0040088

- 581 Fischer, G. a, Gravendeel, B., Sieder, A., Andriantiana, J., Heiselmayer, P., Cribb, P.J., Smidt,  
582 E.D.C., Samuel, R., Kiehn, M., 2007. Evolution of resupination in Malagasy species of *Bulbophyllum*  
583 (Orchidaceae). *Mol. Phylogenet. Evol.* 45, 358–76. doi:10.1016/j.ympev.2007.06.023
- 584 Folk, R. A., Mandel, J. R., & Freudenstein, J. V. (2015). A protocol for targeted enrichment of  
585 intron-containing sequence markers for recent radiations: A phylogenomic example from *Heuchera*  
586 (*Saxifragaceae*). *Applications in Plant Sciences*, 3(8), 1500039.
- 587 Frodin, D.G., 2004. History and concepts of big plant genera. *Taxon* 53, 753–756.  
588 doi:10.2307/4135449
- 589 Gamisch, A., Fischer, G.A., Comes, H.P., 2015. Multiple independent origins of auto-pollination in  
590 tropical orchids (*Bulbophyllum*) in light of the hypothesis of selfing as an evolutionary dead end.  
591 *BMC Evol. Biol.* 15, 192–209. doi:10.1186/s12862-015-0471-5
- 592 Gamisch, A., Comes, H.P., 2019. Clade-age-dependent diversification under high species turnover  
593 shapes species richness disparities among tropical rainforest lineages of *Bulbophyllum*  
594 (Orchidaceae). *BMC Evol. Biol.* 19, 93. doi:10.1186/s12862-019-1416-1
- 595 Garay, L.A., Hamer, F., Siegerist, E.S., 1994. The genus *Cirrhopetalum* and the genera of the  
596 *Bulbophyllum* alliance. *Nord. J. Bot.* 14, 609–646. doi:10.1111/j.1756-1051.1994.tb01080.x
- 597 Gernhard, T., 2008. The conditioned reconstructed process. *J. Theor. Biol.* 253, 769–778.  
598 doi:10.1016/j.jtbi.2008.04.005
- 599 Givnish, T.J., Spalink, D., Ames, M., Lyon, S.P., Hunter, S.J., Zuluaga, A., Doucette, A., Caro, G.G.,  
600 McDaniel, J., Clements, M.A., Arroyo, M.T.K., Endara, L., Kriebel, R., Williams, N.H., Cameron,  
601 K.M., 2016. Orchid historical biogeography, diversification, Antarctica and the paradox of orchid  
602 dispersal. *J. Biogeogr.* 43, 1905–1916. doi:10.1111/jbi.12854
- 603 Givnish, T.J., Spalink, D., Ames, M., Lyon, S.P., Hunter, S.J., Zuluaga, A., Iles, W.J.D., Clements,  
604 M.A., Arroyo, M.T.K., Leebens-Mack, J., Endara, L., Kriebel, R., Neubig, K.M., Whitten, W.M.,  
605 Williams, N.H., Cameron, K.M., 2015. Orchid phylogenomics and multiple drivers of their  
606 extraordinary diversification. *Proc. R. Soc. B Biol. Sci.* 282, 20151553–20151562.  
607 doi:10.1098/rspb.2015.1553
- 608 Górnjak, M., Paun, O., Chase, M.W., 2010. Phylogenetic relationships within Orchidaceae based on  
609 a low-copy nuclear coding gene, *Xdh*: Congruence with organellar and nuclear ribosomal DNA  
610 results. *Mol. Phylogenet. Evol.* 56, 784–95. doi:10.1016/j.ympev.2010.03.003
- 611 Halle, N., 1981. New data and carpograms of orchids from New Caledonia. *Adansonia* 20, 355–368.
- 612 Hassemer, G., Bruun-Lund, S., Shipunov, A. B., Briggs, B. G., Meudt, H. M., & Rønsted, N. (2019).  
613 The application of high-throughput sequencing for taxonomy: the case of *Plantago* subg. *Plantago*  
614 (*Plantaginaceae*). *Molecular phylogenetics and evolution*, 138, 156-173.  
615 doi.org/10.1016/j.ympev.2019.05.013
- 616 Hoang, D.T., Chernomor, O., von Haeseler A., Minh B.Q., and Vinh L.S., 2018. UFBoot2:  
617 Improving the ultrafast bootstrap approximation. *Mol. Biol. Evol.* 35, 518–522.  
618 <https://doi.org/10.1093/molbev/msx281>

- 619 Hosseini, S., Go, R., Dadkhah, K., & Nuruddin, A. A. (2012). Studies on maturase K sequences and  
620 systematic classification of Bulbophyllum in Peninsular Malaysia. *Pak. J. Bot*, 44(6), 2047-2054.
- 621 Hu, A. Q., Gale, S. W., Liu, Z. J., Suddee, S., Hsu, T. C., Fischer, G. A., & Saunders, R. M. (2020).  
622 Molecular phylogenetics and floral evolution of the Cirrhopetalum alliance (Bulbophyllum,  
623 Orchidaceae): Evolutionary transitions and phylogenetic signal variation. *Molecular phylogenetics  
624 and evolution*, 143, 106689.
- 625 IOSPE (2022, 6th July) Internet Orchid Species Photo Encyclopedia. <http://www.orchidspecies.com/>
- 626 Jersáková, J. and Malinová, T., 2007, Spatial aspects of seed dispersal and seedling recruitment in  
627 orchids. *New Phytol.*, 176, 237–241. doi:10.1111/j.1469-8137.2007.02223.x
- 628 Jones, D.L., Clements, M.A., 2001. *Oncophyllum*, a new genus of Orchidaceae from Australia. *The  
629 Orchadian* 13, 420–425.
- 630 Jones, D.L., Clements, M.A., 2002. Nomenclatural changes in the Australian and New Zealand  
631 Bulbophyllinae and Eriinae (Orchidaceae). *The Orchadian* 13, 498–501
- 632 Kalyaanamoorthy S., Minh B.Q., Wong T.K.F., von Haeseler A., and Jermini L.S., 2017.  
633 ModelFinder: fast model selection for accurate phylogenetic estimates. *Nat. Methods*. 14, 587–589.  
634 DOI: 10.1038/nmeth.4285
- 635 Katoh, K., Kuma, K., Toh, H., Miyata, T., 2005. MAFFT version 5: improvement in accuracy of  
636 multiple sequence alignment. *Nucleic Acids Res.* 33, 511–518. doi:10.1093/nar/gki198
- 637 Katoh, K., Misawa, K., Kuma, K., Miyata, T., 2002. MAFFT: a novel method for rapid multiple  
638 sequence alignment based on fast Fourier transform. *Nucleic Acids Res.* 30, 3059–66.
- 639 Kearse, M., Moir, R., Wilson, A., Stones-Havas, S., Cheung, M., Sturrock, S., Buxton, S., Cooper,  
640 A., Markowitz, S., Duran, C., Thierer, T., Ashton, B., Meintjes, P., Drummond, A., 2012. Geneious  
641 Basic: An integrated and extendable desktop software platform for the organization and analysis of  
642 sequence data. *Bioinformatics* 28, 1647–1649. doi:10.1093/bioinformatics/bts199
- 643 Landis, M. J., Matzke, N. J., Moore, B. R., & Huelsenbeck, J. P. (2013). Bayesian analysis of  
644 biogeography when the number of areas is large. *Systematic biology*, 62(6), 789-804.
- 645 Lavarack, B., Harris, W., Stocker, G., 2000. *Dendrobium* and its relatives. Timber Press, Portland.
- 646 Linder, H.P., 1999. *Rytidosperma vickeryae* — a new danthonioid grass from Kosciuszko (New  
647 South Wales, Australia): Morphology, phylogeny and biogeography. *Aust. Syst. Bot.* 12, 743–755.  
648 doi:10.1071/SB97046
- 649 Martin, H.A., 2006. Cenozoic climatic change and the development of the arid vegetation in  
650 Australia. *J. Arid Environ.* 66, 533–563. doi:10.1016/J.JARIDENV.2006.01.009
- 651 Matthews, K.J., Maloney, K.T., Zahirovic, S., Williams, S.E., Seton, M., Müller, R.D., 2016. Global  
652 plate boundary evolution and kinematics since the late Paleozoic. *Glob. Planet. Change* 146, 226–  
653 250. doi:10.1016/J.GLOPLACHA.2016.10.002

- 654 Matzke, N.J., 2013. BioGeoBEARS: Biogeography with Bayesian (and Likelihood) evolutionary  
655 analysis in R Scripts.
- 656 McCormick, M.K., Taylor, D., Juhaszova, K., Burnett, R.K., Whigham, D.F., O'Neill, J.P., 2012.  
657 Limitations on orchid recruitment: not a simple picture. *Mol. Ecol.* 21, 1511–1523.  
658 doi:10.1111/j.1365-294X.2012.05468.x
- 659 Mildenhall, D.C., Kennedy, E.M., Lee, D.E., Kaulfuss, U., Bannister, J.M., Fox, B. and Conran, J.G.,  
660 2014. Palynology of the early Miocene Foulden Maar, Otago, New Zealand: Diversity following  
661 destruction. *Review of Palaeobotany and Palynology*, 204, pp.27-42.
- 662 Minh, B. Q., Nguyen, M. A. T., & von Haeseler, A. (2013). Ultrafast approximation for phylogenetic  
663 bootstrap. *Molecular biology and evolution*, 30(5), 1188-1195.
- 664 Molvray, M., Kores, P.J., Chase, M.W., 1999. Phylogenetic relationships within *Korthalsella*  
665 (Viscaceae) based on nuclear ITS and plastid *trnL-F* sequence data. *Am. J. Bot.* 86, 249–260.  
666 doi:10.2307/2656940
- 667 Nargar, K., O'Hara, K., Mertin, A., Bent, S., Nauheimer, L., Simpson, L., ... & Clements, M. A.  
668 (2022). Evolutionary relationships and range evolution of greenhood orchids (subtribe  
669 Pterostylidinae): insights from plastid phylogenomics. *Front. Plant Sci.* 14, 1063174.  
670 doi.org/10.3389/fpls.2022.912089
- 671 Neubig, K.M., Whitten, A.W.M., Carlswald, B.S., Blanco, M.A., Endara, L., Williams, N.H., Moore,  
672 M., 2008. Phylogenetic utility of *ycf1* in orchids: a plastid gene more variable than *matK*. *Plant Syst.*  
673 *Evol.* 277, 75–84. doi:10.1007/s00606-008-0105-0
- 674 Nguyen, L. T., Schmidt, H. A., Von Haeseler, A., & Minh, B. Q. (2015). IQ-TREE: a fast and  
675 effective stochastic algorithm for estimating maximum-likelihood phylogenies. *Molecular biology*  
676 *and evolution*, 32(1), 268-274. doi.org/10.1093/molbev/msu300
- 677 Peterson, B. K., Weber, J. N., Kay, E. H., Fisher, H. S., & Hoekstra, H. E. (2012). Double digest  
678 RADseq: an inexpensive method for de novo SNP discovery and genotyping in model and non-  
679 model species. *PloS one*, 7(5), e37135.
- 680 Pridgeon, A.M., Cribb, P.J., Chase, M.W., Rasmussen, F.N., 2014. Genera Orchidacearum Volume 6  
681 Epidendroideae. Oxford University Press, New York, USA.
- 682 Puente-Lelièvre, C., Harrington, M.G., Brown, E.A., Kuzmina, M., Crayn, D.M., 2013. Cenozoic  
683 extinction and recolonization in the New Zealand flora: The case of the fleshy-fruited epacrids  
684 (Styphelieae, Styphelioideae, Ericaceae). *Mol. Phylogenet. Evol.* 66, 203–214.  
685 doi:10.1016/J.YMPEV.2012.09.027
- 686 Drummond, A. J., & Rambaut, A. (2007). BEAST: Bayesian evolutionary analysis by sampling trees.  
687 *BMC evolutionary biology*, 7(1), 1-8.
- 688 Rambaut, A., Drummond, A.J., 2007. Tracer v.1.5. Available from: <http://beast.bio.ed.ac.uk/Tracer>
- 689 Ree, R.H., Smith, S.A., 2008. Maximum likelihood inference of geographic range evolution by  
690 dispersal, local extinction, and cladogenesis. *Syst. Biol.* 57, 4–14. doi:10.1080/10635150701883881

- 691 Ronquist, F., 1997. Dispersal-vicariance analysis: a new approach to the quantification of historical  
692 biogeography. *Syst. Biol* 46, 195–203.
- 693 Ronquist, F., 2001. DIVA version 1.2. Computer program for MacOS and Win32.
- 694 Sanmartín, I., Wanntorp, L., Winkworth, R.C., 2007. West Wind Drift revisited: testing for  
695 directional dispersal in the Southern Hemisphere using event-based tree fitting. *J. Biogeogr.* 34, 398–  
696 416. doi:10.1111/j.1365-2699.2006.01655.x
- 697 Sansaloni, C., Petrolí, C., Jaccoud, D., Carling, J., Detering, F., Grattapaglia, D., & Kilian, A. (2011).  
698 Diversity Arrays Technology (DARt) and next-generation sequencing combined: genome-wide, high  
699 throughput, highly informative genotyping for molecular breeding of Eucalyptus. In *BMC*  
700 *proceedings* (Vol. 5, No. 7, pp. 1-2). BioMed Central.
- 701 Serna-Sánchez, M. A., Pérez-Escobar, O. A., Bogarín, D., Torres-Jimenez, M. F., Alvarez-Yela, A.  
702 C., Arcila-Galvis, J. E., ... & Arias, T. (2021). Plastid phylogenomics resolves ambiguous  
703 relationships within the orchid family and provides a solid timeframe for biogeography and  
704 macroevolution. *Scientific reports*, 11(1), 1-11.
- 705 Schmidt-Lebuhn, A. N., Egli, D., Grealy, A., Nicholls, J. A., Zwick, A., Dymock, J. J., & Gooden, B.  
706 (2022). Genetic data confirm the presence of *Senecio madagascariensis* in New Zealand. *New*  
707 *Zealand Journal of Botany*, 1-13.
- 708 Simpson, L., Clements, M.A., Crayn, D.M., Nargar, K., 2018. Evolution in Australia’s mesic biome  
709 under past and future climates: insights from a phylogenetic study of the Australian Rock Orchids  
710 (*Dendrobium speciosum* complex, Orchidaceae). *Mol. Phylogenet. Evol.* 118, 32–46.  
711 doi:10.1016/J.YMPEV.2017.09.004
- 712 Smidt, E.C., Gallo, L.W., Scatena, V.L., 2013. Leaf anatomical and molecular studies in  
713 *Bulbophyllum* section *Micranthae* (Orchidaceae) and their implications for systematics. *Brazilian J.*  
714 *Bot.* 36, 75–82. doi:10.1007/s40415-013-0008-3
- 715 Smidt, E.C., Borba, E.L., Gravendeel, B., Fischer, G.A., Berg, C. Van Den, 2011. Molecular  
716 phylogeny of the Neotropical sections of *Bulbophyllum* (Orchidaceae) using nuclear and plastid  
717 spacers. *Taxon* 60, 1050–1064.
- 718 Sun, Y., Skinner, D.Z., Liang, G.H., Hulbert, S.H., 1994. Phylogenetic analysis of *Sorghum* and  
719 related taxa using internal transcribed spacers of nuclear ribosomal DNA. *Theor. Appl. Genet.* 89,  
720 26–32. doi:10.1007/BF00226978
- 721 Swenson, U., Backlund, A., McLoughlin, S., Hill, R.S., 2001. *Nothofagus* biogeography revisited  
722 with special emphasis on the enigmatic distribution of subgenus *Brassospora* in New Caledonia.  
723 *Cladistics* 17, 28–47. doi:10.1111/j.1096-0031.2001.tb00109.x
- 724 Szlachetko, D.L., Margonska, H.B., 2001. Genera et species *Orchidialium*. 3. *Polish Bot. J.* 461, 113–  
725 121.
- 726 Pérez-Escobar, O.A., Chomicki, G., Condamine, F.L., Karremans, A.P., Bogarín, D., Matzke, N.J.,  
727 Silvestro, D., Antonelli, A., 2017. Recent origin and rapid speciation of Neotropical orchids in the  
728 world’s richest plant biodiversity hotspot. *New Phytol.* 215, 891–905. doi:10.1111/nph.14629

- 729 Van den Berg, C. 2003. Estudos em sistemática molecular na família Orchidaceae. Thesis presented  
730 for obtaining the title of Full Pro-fessor, Universidade Estadual de Feira de Santana, Bahia, Brazil.
- 731 van Kleinwee, I., Larridon, I., Shah, T., Bauters, K., Asselman, P., Goetghebeur, P., ... & Veltjen, E.  
732 (2022). Plastid phylogenomics of the Sansevieria Clade of Dracaena (Asparagaceae) resolves a recent  
733 radiation. *Molecular Phylogenetics and Evolution*, 107404. doi:10.1016/j.ympev.2022.107404
- 734 Vermeulen, J.J., 1993. A taxonomic revision of *Bulbophyllum* sections *Adelopetalum*, *Lepanthanthe*,  
735 *Macrouris*, *Pelma*, *Peltopus*, and *Unicifera* (Orchidaceae). Orchid Monogr. 7.
- 736 Vermeulen, J.J., Schuiteman, A., De Vogel, E.F., 2014. Nomenclatural changes in *Bulbophyllum*  
737 (Orchidaceae; Epidendroideae). *Phytotaxa* 166, 101–113. doi:10.11646/phytotaxa.166.2.1
- 738 Wagstaff, S.J., Bayly, M.J., Garnock-Jones, P.J., ip Garnock-Jones, P.J., Albach, D.C., 2002.  
739 Classification, origin, and diversification of the New Zealand *Hebes* (Scrophulariaceae). *Ann.*  
740 *Missouri Bot. Gard.* 89, 38–63.
- 741 Wagstaff, S.J., Breitwieser, I., Swenson, U., 2006. Origin and relationships of the Austral genus  
742 *Abrotanella* (Asteraceae) inferred from DNA sequences. *Taxon* 55, 95–106. doi:10.2307/25065531
- 743 Wagstaff, S.J., Dawson, M.I., Venter, S., Munzinger, J., Crayn, D.M., Steane, D.A., Lemson, K.L.,  
744 2010. Origin, diversification, and classification of the Australasian genus *Dracophyllum* (Richeeae,  
745 Ericaceae). *Ann. Missouri Bot. Gard.* 97, 235–258. doi:10.3417/2008130
- 746 Weitemier, K., Straub, S. C., Cronn, R. C., Fishbein, M., Schmickl, R., McDonnell, A., & Liston, A.  
747 (2014). Hyb-Seq: Combining target enrichment and genome skimming for plant phylogenomics.  
748 *Applications in plant sciences*, 2(9), 1400042.
- 749 WCSP (6<sup>th</sup> July, 2022). World Checklist of Selected Plant Families. *Facilitated by the Royal Botanic*  
750 *Gardens, Kew.* <http://wcsp.science.kew.org/> Retrieved 2022, 6<sup>th</sup> July.
- 751 Weising, K., Nybom, H., Pfenninger, M., Wolff, K., Kahl, G., 2005. DNA fingerprinting in plants:  
752 principles, methods, and applications 2nd. ed. CRC Press, BocaRaton, Florida.
- 753 Yu, Y., Harris, A.J., Blair, C., He, X., 2015. RASP (Reconstruct Ancestral State in Phylogenies): A  
754 tool for historical biogeography. *Mol. Phylogenet. Evol.* 87, 46–49.  
755 doi:10.1016/J.YMPEV.2015.03.008
- 756 Yule, G.U., 1925. A Mathematical Theory of Evolution, Based on the Conclusions of Dr. J. C.  
757 Willis, F.R.S. *Philos. Trans. R. Soc. B Biol. Sci.* 213, 21–87. doi:10.1098/rstb.1925.0002
- 758 Zahirovic, S., Matthews, K. J., Flament, N., Müller, R. D., Hill, K. C., Seton, M., & Gurnis, M.  
759 (2016). Tectonic evolution and deep mantle structure of the eastern Tethys since the latest Jurassic.  
760 *Earth-Science Reviews*, 162, 293-337.
- 761 Zuckerkandl, E., Pauling, L., 1965. Molecules as documents of evolutionary history. *J. Theor. Biol.*  
762 8, 357–366. doi:10.1016/0022-5193(65)90083-4